Monodisperse Rodlike Oligomers and Their Mesomorphic Higher Molecular Weight Homologues†

Shaul M. Aharoni

Engineered Materials Sector Laboratory, Allied/Signal Corporation, Morristown, New Jersey 07960. *Received January 19, 1987*

ABSTRACT: Monodisperse aromatic amide rodlike oligomers were prepared together with several higher molecular weight poly(*p*-benzanilide terephthalamide) (p-BT) homologues. For comparison, several molecular weight fractions each of poly(*p*-benzamide) (p-BA) and poly(*p*-benzanilide nitroterephthalamide) (p-BNT) were also prepared. Dilute solutions of the monodisperse oligomers showed a dependence of the intrinsic viscosity on M_w to a power of 0.79. The higher molecular weight p-BT showed a power dependence greater than 1.0, as usual for rodlike molecules. p-BA and p-BNT showed similar power dependence. All these are far less than the theoretical expectation. Also unusual were the extremely high values of the Huggins coefficient, k_H, exhibited by the monodisperse oligomers. Concentrated solutions of the polymers and oligomers with axial ratio $x \geq 7$ showed lyotropic liquid crystallinity. When $x \leq 6$, no liquid crystallinity was obtained. Thermal studies on bulk p-BT and the oligomers indicate thermotropic liquid crystallinity for the oligomer with $x = 7$, in support of the observations in concentrated solutions. The polymeric crystal structure of p-BT is remarkably similar to those of p-BA and p-PT and is fully developed in oligomers with $x \geq 6$. Similarities to the pattern of high-M p-BT become noticeable in WAXD patterns of oligomers with x as small as 3.

Introduction

The specific viscosity of dilute polymer solutions, η_{sp}, is defined as

$$\eta_{sp} = \frac{\eta_0 - \eta_s}{\eta_s} = \frac{\eta_0}{\eta_s} - 1 = \nu c \tag{1}$$

where η_0 is the solution viscosity at zero shear, η_s is the solvent viscosity, c is the volume fraction of the solute, and ν is a shape factor. Rearrangement and extrapolation to zero concentration yields the intrinsic viscosity $[\eta]$ of the polymer:

$$[\eta] = \left(\frac{\eta_0 - \eta_s}{\eta_s c}\right)_{c \to 0} = \nu \tag{2}$$

For impenetrable spheres, $[\eta] = \nu = 2.5$. Conversion to the commonly used viscosity unit of dL/g changes the value of $[\eta] = \nu$ to 0.025. Prolate ellipsoids of revolution are commonly used to represent slender rodlike solute particles. In this case, $[\eta] = \nu$ increases with the axial ratio, x, defined as

$$x = L/d \tag{3}$$

where L is the length of the particle and d is its diameter.

It has been shown by Tanford[1] that the axial ratio of a cylindrical rod is 1.225 $(1/(2/3)^{1/2})$ times larger than the axial ratio of a prolate ellipsoid of the same volume. In light of this relatively small difference, the effects of conversion from rodlike molecules to the prolate ellipsoid model were neglected in this work.

It is well-known that the empirical Mark–Houwink equation

$$[\eta] = KM^a \tag{4}$$

relating the intrinsic viscosity, $[\eta]$, to the molecular weight, M, reflects the chain expansion of the polymer through the magnitude of the exponent a. Thus, when the polymeric solute particles behave as hard impenetrable spheres, $a = 0$, and when the solute particles are infinitely long monodisperse rods, $a = 2.0$. In the case of flexible coil polymers, $a = 0.5$ under Θ-conditions and approaches 0.8 with improved solvent quality and the resultant coil expansion. It is well accepted that when a significantly surpasses 1.0, an extended chain behavior is evidenced, with rodlike behavior being closer and closer approximated as the magnitude of a increases toward 2.0. It has been shown theoretically as well as experimentally that this limit is dependent on the chain length (L) and the axial ratio (x) of the rodlike particles, decreasing somewhat below 2.0 as L decreases from infinity into the realm of experimentally available polymers:[2]

$$[\eta] \propto L^2/\log x \tag{5}$$

This proportionality is in agreement with the asymptotic form of Simha's formula for a prolate ellipsoid with $x \gg 1$:[3]

$$\nu = \frac{x^2}{15(\log 2x - 3/2)} + \frac{x^2}{5(\log 2x - 1/2)} + \frac{14}{15} \tag{6}$$

In a subsequent numerical treatment, Simha and associates[4] calculated the values of ν for prolate ellipsoids with axial ratios $1.0 \leq x \leq 300$. When the calculated ν values (or the identical $[\eta]$ values) are plotted on log–log paper against x or against the corresponding M values, one finds the relationship to be described by a curve with two branches smoothly connected over a wide range of x. In the high-x or high-M branch, the data points fall on a straight line with a slope of $a = 1.72$. This is, of course, as expected for this range of axial ratios.[4,5] For axial ratios in the range $10^6 \leq x \leq 10^9$, we calculated the slope to be $a = 1.90$. However, for small x values, say below $x = 10$, the curve defined by the calculated points is not linear and its tangential slope decreases with diminishing x to substantially below 1.0. We are confronted with the unusual situation that for prolate ellipsoids approximating rodlike molecules with axial ratios smaller than about 10, the exponent a in the Mark–Houwink equation (eq 4) is significantly smaller than 1.0. The question arises: is this an experimentally verifiable fact, supporting Simha's seminal work, or is it a mathematical artifact caused by the model selected to represent rodlike macromolecules? Part of the work in this paper tackles this problem.

To obtain good viscosity data for the low-M branch of the $[\eta]$–x curve, it is preferable to use solute molecules with all the following. (a) Solute must be highly soluble in solvent with no molecular aggregation. (b) Solute molecules must be of identical length; i.e., each oligomeric fraction must be monodisperse. (c) Solute molecules must be rodlike in solution or as close as possible to it. (d) Solute molecules should not exhibit a polyelectrolyte effect in

† Dedicated to Professor Robert Simha on the occasion of his 75th birthday.

0024-9297/87/2220-2010$01.50/0

solution; this may be achieved by the molecules having no strongly ionizable entities such as reactive end groups. The requirements of monodispersity and absence of ionizable groups may be relaxed for higher molecular weight fractions, in the high-M branch and transition interval of the $[\eta]$–x or $[\eta]$–M curve.

The above prerequisites were all met by synthesizing monodisperse para-substituted aromatic polyamide oligomers having rodlike shape whose ends are capped by phenyl groups

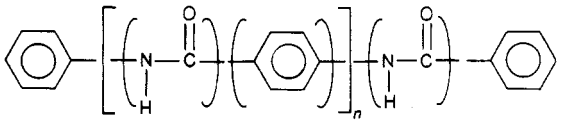

with n = 0–5. Three kinds of higher molecular weight polymers were prepared in order to study the high-M branch and transition interval. None was monodisperse or end capped as the low-M oligomers. The first higher M polymer prepared is poly(*p*-benzanilide terephthalamide) (p-BT) of various molecular weights:

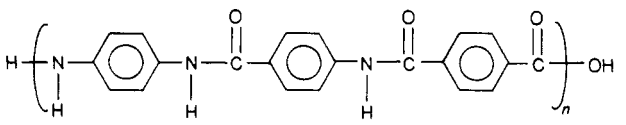

Structurally, these are closest to the monodisperse oligomers. The second polymer series was poly(*p*-benzanilide nitroterephthalamide) (p-BNT):

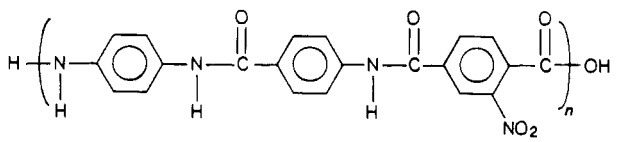

The third series of variable molecular weight polymers was the poly(*p*-benzamide) (p-BA):

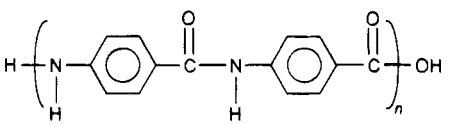

In addition to our own viscosity results, literature data obtained from p-BA and poly(*p*-phenylene terephthalamide) (p-PT) solutions were considered in comparing the theoretical to experimental results in the high-M branch of the $[\eta]$–M curves.

The behavior of relatively short rodlike particles at the other end of the concentration spectrum is most interesting. In the bulk or concentrated solution, such particles exhibit liquid crystalline behavior provided their axial ratio surpasses a certain critical value, x_c. In his original treatment of the problem, Flory calculated in 1956 that in the bulk, $x_c = 6.7$.[6] Later this value was revised slightly downward, to $x_c = 6.4$.[7,8] This critical axial ratio is taken to be valid for monodisperse rods not connected to one another. The cases where rodlike segments of a macromolecule are connected along the chain by joints of variable flexibility were treated by Flory[9] and Matheson and Flory,[10] with the results that in the connected rods ensemble, x_c becomes substantially smaller than in the unconnected case. This is in agreement when experimental observations indicating that x_c decreases with increased flexibility of the joints or flexible spacers along the chain. This reduction in x_c progresses from $5 < x_c < 6$ for tetrahedral bond angle about a single atom[11] to $3 < x_c < 3.5$ for highly flexible spacers, allowing for complete directional independence of one rodlike segment from its neighbors along the chain.[12]

When tested experimentally, it was found[8] that the onset of thermotropic mesomorphicity occurs at $x_c \geq 5.0$ for monodisperse poly-*p*-phenylene oligomers. This x_c value is somewhat lower than theoretically expected. In the present work, the value of x_c for monodisperse poly(*p*-phenylene amide) oligomers is determined and compared with theory. In addition, some solid-state properties of the monodisperse oligomers will be described, compared with the higher M homologues, and discussed.

Experimental Section

The lowest homologue in the series of monodisperse phenyl end-capped aromatic amide oligomers is benzanilide (MW = 196)

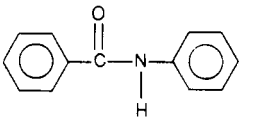

which was obtained from Aldrich Chemical Co. In addition, the oligomers in Chart I were prepared in our laboratory in one or more steps leading to a single monodisperse product at the end of the synthetic sequence. Specifically, the synthetic procedure was as follows. For *p*-triphenylene diamide (MW = 315), aniline was reacted with terephthalic acid according to the Yamazaki[13] (Y) procedure or, alternatively, with terephthaloyl chloride under Schotten–Baumann (SB) conditions. Benzoic acid was reacted under Y conditions with 4,4′-diaminobenzanilide to obtain *p*-tetraphenylene triamide (MW = 434). For *p*-pentaphenylene tetraamide (MW = 553), 4-aminobenzanilide was reacted with terephthalic acid according to the Y procedure. To obtain *p*-hexaphenylene pentaamide (MW = 672), benzoyl chloride was reacted with *p*-aminobenzoic acid under SB conditions, and the product was then reacted with 4,4′-diaminobenzanilide under Y conditions. The *p*-heptaphenylene hexaamide (MW = 791) was made by reacting terephthaloyl chloride with *p*-aminobenzoic acid under SB conditions and then using the Yamazaki procedure to react the product with 4-aminobenzanilide.

Higher molecular weight polyamides were all prepared by the Yamazaki[13] procedure. These were not end capped. Increasing molecular weights were obtained by allowing the reaction to progress for increasing time durations prior to quenching and workup. p-BA was made from *p*-aminobenzoic acid. p-BT and p-BNT were made from 4,4′-diaminobenzanilide and terephthalic acid or nitroterephthalic acid, respectively.

Reagents were used as obtained from chemical supply houses. 4,4′-Diaminobenzanilide was obtained from Sandoz Colors and Chemicals and was recrystallized from methanol/acetone prior to use. Pyridine and *N*,*N*-dimethylacetamide (DMAc) were stored over molecular sieves before use. The concentrated sulfuric acid used as solvent was 96% in strength.

The structure of all polymers and monodisperse oligomers was confirmed by carbon-13 NMR spectra obtained with a Varian XL-200 Fourier Transform NMR spectrometer from about 10% solutions in concentrated H_2SO_4. Light-scattering studies of solutions of p-BT and p-BA in DMAc containing 5% LiCl (DMAc/LiCl) showed clear evidence of molecular aggregation. Therefore, the molecular weight determinations of these polymers were conducted in concentrated H_2SO_4 solutions, where no aggregation could be detected. The weight-average molecular weight, M_w, of the monodisperse oligomers and higher M p-BT homologues was determined by small volume static light-scattering measurements using a Langley Ford multiangle photon correlation instrument. The M_w's of p-BA and of p-BNT were determined by low-angle laser light-scattering measurements in a Chromatix KMX-6 instrument. For p-BA, concentrated H_2SO_4 was used as solvent, and for p-BNT, DMAc/LiCl was used. All the solutions were carefully centrifuged and then filtered through fluoropore filters with pore diameters of 0.2 μm, prior to the M_w determinations.

Because of its solubility in DMAc/LiCl, the number-average molecular weight, M_n, of the various p-BNT homologues was determined by titration of amine and carboxyl end groups. In all cases, the M_w/M_n ratio was 1.5 ± 0.05.

Dilute solution (≤2%) viscosities were measured at 25 °C on solutions of all monodisperse oligomers and polymers in con-

Chart I

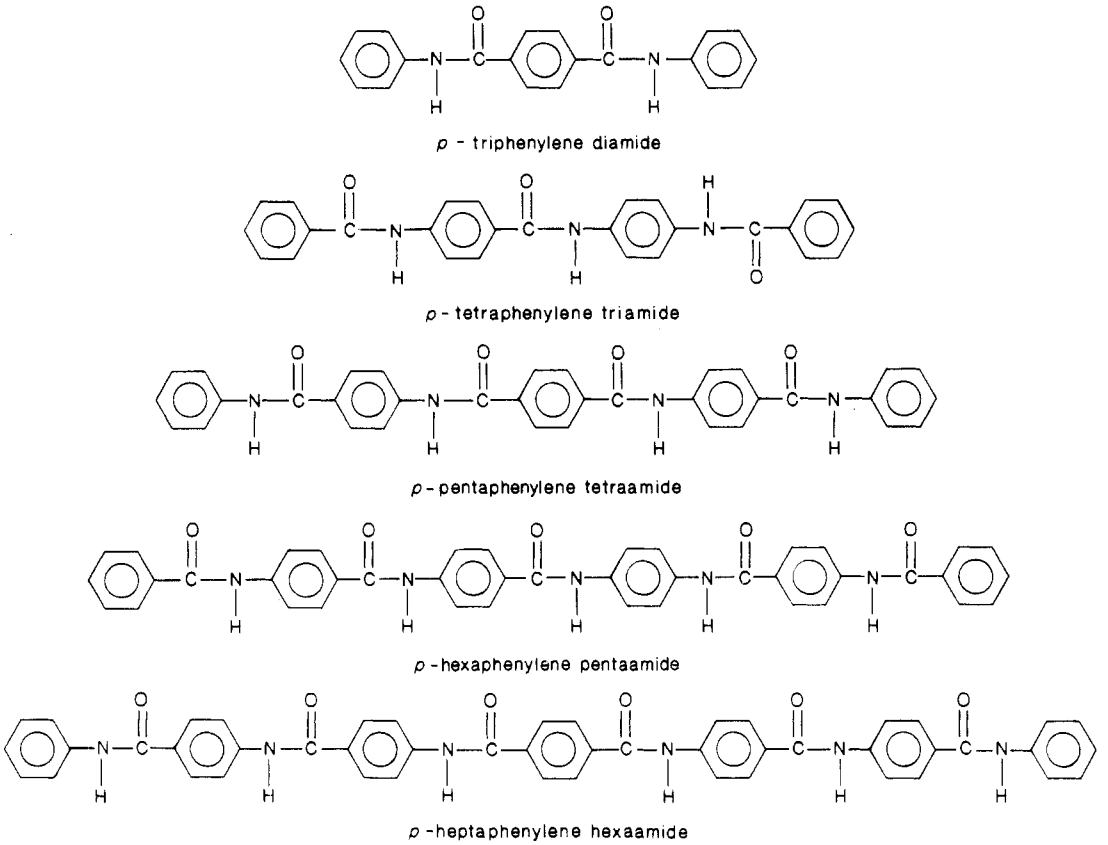

Table I
Intrinsic Viscosity-M_w Relationships[a]

polymer	ref	range	K	a	r
p-BT	TW	$M_w < 1000$	4.27×10^{-4}	0.793	0.9988
p-BT	TW	$1800 \leq M_w \leq 18\,500$	5.25×10^{-5}	1.217	0.9890
p-BA	TW	$3100 \leq M_w \leq 13\,000$	2.14×10^{-5}	1.203	0.9974
p-BA	16	$5300 \leq M_w \leq 51\,000$	1.67×10^{-5}	1.234	0.9794
p-BA	17	$7140 \leq M_w \leq 23\,000$[b]	2.69×10^{-6}	1.406	0.9091
p-BNT	TW	$2000 \leq M_w \leq 27\,500$	5.93×10^{-5}	1.068	0.9999
p-PT	16	$7000 \leq M_w \leq 125\,000$	7.90×10^{-5}	1.062	0.9816
p-PT	18	$1680 \leq M_w \leq 63\,000$	7.85×10^{-5}	1.092	0.9978
p-PT	19	$4500 \leq M_w \leq 45\,000$	1.49×10^{-5}	1.237	0.9858
p-PE	20	$318 \leq M_w \leq 558$	3.02×10^{-3}	0.483	0.9949
p-PE	20	$5500 \leq M_w \leq 27\,200$[c]	2.04×10^{-5}	1.126	0.9666

[a] Viscosities are in dL/g units. Viscosities of p-BT, p-BA, p-BNT, and p-PT were measured in concentrated H_2SO_4. Viscosities of p-PE were measured in dichloroacetic acid. TW = this work. [b] Molecular weight as determined from flow birefringence and sedimentation studies. [c] Twelve experimentally determined polymer fractions were used to obtain K, a, and r in this system.

centrated sulfuric acid, using Cannon-Ubbelohde internal dilution glass viscometers with solvent efflux time between 100 and 500 s.

Wide-angle X-ray diffraction (WAXD) patterns were obtained from the pulverized materials at ambient temperature by using a Philips X-ray diffractometer operating in parafocus geometry with monochromatized Cu Kα radiation. Thermal studies were conducted by using a Du Pont model 9900 thermogravimetric analyzer (TGA) and differential scanning calorimeter (DSC) at a heating rate of 20 K/min, under argon or nitrogen atmosphere, respectively. Cross-polarized light microscopy studies were conducted by using an Olympus BH-2 microscope equipped with a Reichert hot stage capable of reaching ~390 °C. This temperature was found to be lower than the transition temperatures of *p*-heptaphenylene hexaamide. To study this oligomer, it was sealed under nitrogen in a melting point capillary glass tube. The tube was heated on a thermostated hot plate to about 450 °C and immediately transferred to the fully heated microscope hot stage for observation. Alternatively, the tube was either quenched or allowed to slowly cool to room temperature prior to the cross-polarized light microscopy observations. Densities were measured pycnometrically in mixtures of CCl_4 and hexane.

From data collected by Aharoni,[14,15] one calculates that for para-substituted aromatic polyamides, the axial ratio per ring is very close to unity. Therefore, in this paper the axial ratio per aromatic ring is approximated by 1.0 throughout.

Results and Discussion

Dilute Solutions. The intrinsic viscosities in concentrated H_2SO_4 of all oligomers and polymers prepared by us are logarithmically plotted in Figure 1 against their M_w, obtained from light-scattering measurements, and the corresponding axial ratios. The values of K and a in eq 4 were obtained from the numerical data by least-squares curve fitting of all the points within each homologous family. For each such series of data, the correlation coefficient, r, was also calculated. It is tabulated in Table I together with the values of K and a and the M_w range for which the correlations were determined. Several pairs of K and a values were determined by us from literature data for p-PT, p-BA, and a mainly para aromatic polyester (p-PE) and are presented in Table I for comparison.

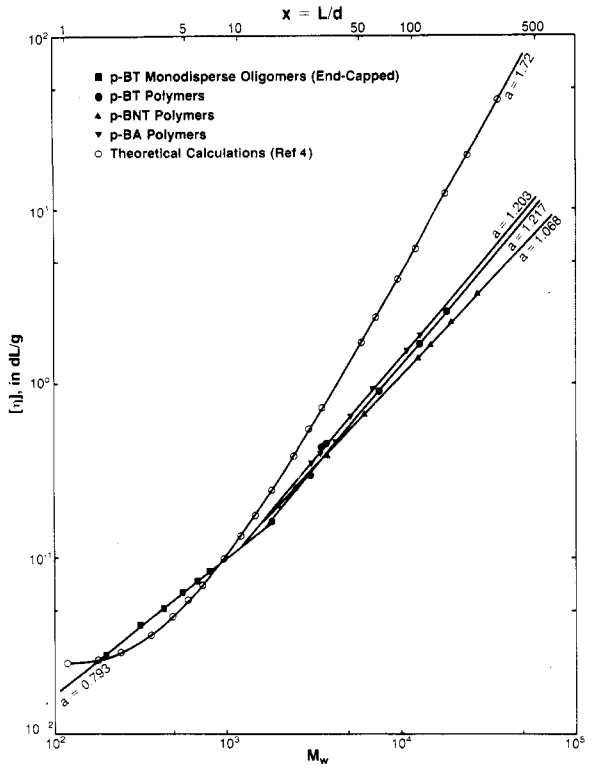

Figure 1. Theoretical and experimental (in concentrated H_2SO_4) intrinsic viscosities of rodlike polymers plotted on log–log paper against M_w and the axial ratio x.

Occasionally, the values of K and a determined by us from raw literature data were different from the corresponding values given in the original publication, but since they were determined numerically and not graphically, we believe our values to be the correct ones. Importantly, no polyelectrolyte effect or molecular aggregation behavior was observed in any of our viscosity studies in concentrated sulfuric acid.

In addition to the experimental data, the theoretical intrinsic viscosity values calculated by Mehl et al.[4] for prolate ellipsoids with $1 \leq x \leq 300$ are shown in Figure 1. The experimental data in the figure are easily separable into two branches. The low molecular weight monodisperse end-capped oligomers fall on a straight line whose slope is $a = 0.793$. This is in reasonable agreement with the theoretical values for $x < 10$. These fall on a curve whose tangential slope diminishes to substantially less than 1.0 as x becomes smaller. It should be recognized that the actual differences between calculated and measured intrinsic viscosities in this range are very small, of the order of 0.005 dL/g.

The most striking observation of the dilute solution study is the low power dependence of the low-M branch of the $[\eta]$–M_w curve. This is in general agreement with the prediction of Simha.[3,4] It is also in agreement with the very low power dependence of monodisperse oligomeric polyesters observed by Tsvetkov et al.,[20] but their results are based on only two fully para-substituted oligomers.

Above a transition interval of about $10 \leq x < 15$, the theoretical and experimental results all fall on straight lines. The slopes of the experimental lines fall in the interval $1.068 \leq a \leq 1.217$, substantially lower than the theoretical $a = 1.72$ slope. Additional literature results, in Table I, also indicate a to be significantly smaller than the theoretical value for rigid prolate ellipsoids with large x. Experimental results in the literature with a values larger than theoretically expected may be explained as due mostly to molecular aggregation effects.

The quality of the data in the high-M branches of the $[\eta]$–M_w curves is most instructive. In our own case, we have used the same concentrated sulfuric acid for all viscosity and light-scattering measurements. Therefore, the different slopes obtained from viscosity measurements must reflect the nature of the investigated polymers and cannot be attributed to differences in the strength of the sulfuric acid. In our case, the slopes of the p-BT and p-BA polymers are essentially identical, indicating that the differences between these polymers are apparently too slight to be reflected by meaningful changes in a. We believe the same argument also holds for the great similarity between p-BA and p-PT. The slope for the p-BNT series is somewhat lower, probably reflecting the higher flexibility of the p-BNT chain.[21] We cannot claim use of the same H_2SO_4 for other polymers in Table I and must conclude that differences in the values of a obtained by different groups may reflect differences in the strength of the H_2SO_4 used by them, in addition to variations in chain rigidity when applicable. In fact, Baird and Smith[22] report substantial changes in the viscosity of p-PT upon changing the strength of the sulfuric acid from 96.6% to 105.0%.

In light of the data in Table I, Figure 1, and the above discussion, we believe that in the absence of aggregation and/or polyelectrolyte effects, it is highly improbable to obtain values of a close to 1.7 or above it, as is occasionally claimed in the literature. Such high values require individual rodlike molecules of very large axial ratio behaving in a perfectly rigid manner. We do not believe any of the presently available "rodlike" macromolecules fulfills these requirements.

It is of interest to note that the lines of the high-M branches in Figure 1 appear to converge in the transition interval right when they are about to merge with the low-M branch of the $[\eta]$–x curve. The area of convergence and merging is at about $10 \leq x < 13$, corresponding to $1150 \leq M_w < 1550$ with two of the three lines merging at the lower end of this M_w range. This is very close to the molecular weight between entanglements, M_c, of 1180 estimated for p-PT by Baird and Ballman.[23] The significance of this observation eludes us at present.

From the above, one concludes that in the low-M branch of the $[\eta]$–M_w curve, $a < 1.0$, and above the convergence interval $1.0 < a < 1.7$. We speculate that when the rodlike oligomers are very short, the measured viscosity reflects only the general shape of the rodlike entity. In the high-M branch, the viscosity also reflects differences between relatively rigid macromolecules, provided the differences are substantial.

In order to keep the solution efflux time during viscosity measurements within the range of 100–500 s, the glass viscometers were changed with changes in solution concentration. The usual curves of reduced viscosity, η_{sp}/c, plotted against concentration were all straight lines and showed no breaks at the points where the glass viscometers were changed. This indicates that for the oligomers and polymers in this study, the orientational relaxation during the viscosity measurements was sufficiently rapid to keep the rodlike molecules randomly oriented in the solvent. Only at substantially higher concentrations, which depend on the axial ratios of the solute particles, do molecular orientation effects due to changes in the viscometer capillary diameter and consequent shear rate become noticeable.

If the reduced viscosity data in the concentration interval $0.125 \leq c \leq 2.0\%$ are used and the Huggins equation[24] is employed

$$(\eta_0 - \eta_s)/\eta_s c = \eta_{sp}/c = [\eta] + k_H[\eta]^2 c \qquad (7)$$

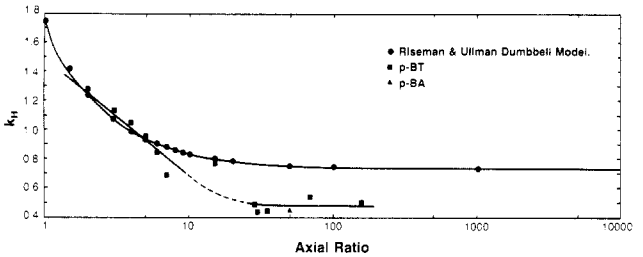

Figure 2. Theoretical and experimental (in concentrated H_2SO_4) values of the Huggins parameter k_H of rodlike polymers, plotted on semilog paper against the axial ratio x.

the Huggins parameter k_H, reflecting the hydrodynamic influence of increased concentration on solution viscosity, was calculated for all monodisperse oligomers and many of their higher M homologues. The results are divisible into two groups. In the higher molecular weight range, where the axial ratio, x, is larger than 20, the values of k_H for all polymers in this study fall in the interval of 0.44–0.54. In the low molecular weight region, where $2 \leqslant x \leqslant 13$, the values of k_H continuously increase as x decreases. The data, presented in Figure 2, show some scatter, but in light of the notoriously high scatter usually found among k_H values, the trends are gratifyingly clear. In the same figure are plotted points calculated for the dumbbell molecule model of Riseman and Ullman[25] according to which

$$k_H \simeq (11/15)(1 + 311d/225L) \quad (8)$$

For an infinitely long dumbbell, this value asymptotically approaches $11/15 = 0.7333$ which is the k_H determined[25] for the rigid rod molecule. Simha's treatment of solutions of dumbbell molecules yields $k_H = 0.77$.[26] For a flexible, randomly (centrosymmetric) coiled molecule, Riseman and Ullman[25] assert $k_H = 0.600$. An important fact to realize is that in the Riseman and Ullman dumbbell model, the value of k_H is axial ratio dependent, while neither the random coil nor the rodlike particle models are. The rodlike limit of the dumbbell model was previously recognized by Riseman and Kirkwood.[27] In the region of small axial ratios, good agreement between the experimental values and the theoretical expectations is especially instructive and, we believe, valid in light of the fact that the prolate ellipsoid model range of applicability covers the small-x region.[3-5] An overall agreement between both models is expected since both the prolate ellipsoid and dumbbell models are meant to describe the behavior during flow and the viscosity of dilute solutions of rodlike molecules with varying axial ratios. In the region where the axial ratio is large, say at $x \geqslant 20$, the experimental data are significantly and consistently smaller than theory. Such a difference is well-known for practically all flexible coil polymers and is probably due to reduced hydrodynamic interactions[26] between solute particles. The important conclusion is, however, the obvious trend of increasing k_H with decreasing x in the low-x region, a trend appearing both experimentally and in the Riseman and Ullman[25] dumbbell model. The increased k_H is due, naturally, to the increased draining of the shorter rods and the ensuing larger hydrodynamic interactions between them.

Concentrated Solutions. When the concentration of long rigid rodlike or semirigid polymeric molecules in an isotropic solution is gradually increased, a point is reached at C_c, where an anisotropic liquid phase separates out. At even higher concentrations, the isotropic solution diminishes in volume and the anisotropic solution increases, until

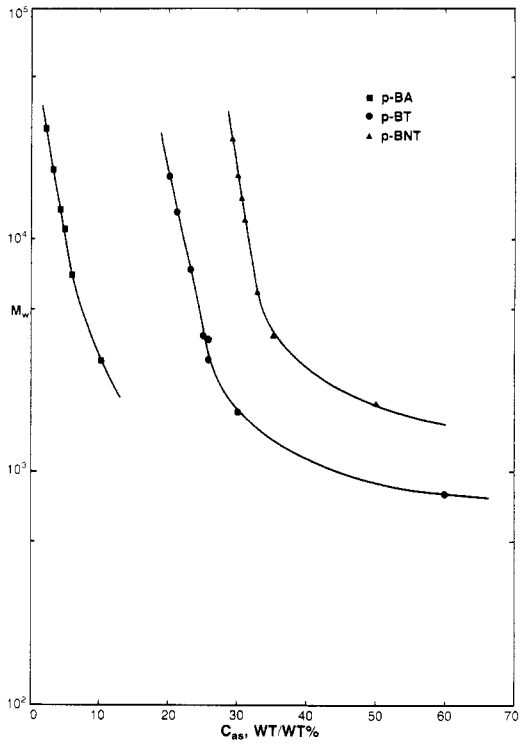

Figure 3. Onset of apparently single-phase lyotropic liquid crystallinity at the concentration C_{as}, plotted on semilog paper against M_w. All result obtained in concentrated sulfuric acid.

a point is reached where only a single-phase anisotropic solution is present. The polymer concentration at this point will be denoted below by C_{as}. The systems prepared by us, namely p-BT, p-BA, and p-BNT, all exhibit an anisotropic liquid crystalline phase, as well as a biphasic interval at concentrations between C_c and C_{as}. The results of our determinations of C_{as} for members of the three families above are plotted as function of M_w in Figure 3.

Now, the chain rigidity of rigid or semirigid rodlike macromolecules is often inferred in the literature from the persistence length, q, or the Kuhn segment length, A, of the chain: the larger these parameters are, the closer is the chain to strict rodlike behavior. Light-scattering studies gave the values of $q \cong 500$ and 175 Å for p-BA and p-PT, respectively.[18] For p-BNT we estimated[21,28] a q value of around 100 Å. A glance at Figure 3 clearly reveals that the position of the C_{as} curves of the three polymeric families is linked to their backbone rigidity. The stiffer the chain, the lower the concentration C_{as}.

The molecular weight or axial ratio dependence of C_{as} is rather weak in the higher M branch of the data. In general, a break in the curve occurs at $x \lesssim 15$ and a much stronger dependence of C_{as} on x is clearly evident. We have insufficient data to demonstrate this point conclusively, but the trend is evident in all three series: p-BA, p-BT, and p-BNT. In fact, in the case of the p-BT monodisperse oligomers, we could not induce lyotropic liquid crystallinity in any member whose $x \leqslant 6$ at any solution (both sulfuric acid and DMAc/5% LiCl) concentration and observed lyotropic liquid crystallinity only in the $x = 7$ case. The question of what is the critical axial ratio, x_c, below which liquid crystallinity does not exist will be addressed in the following section.

Cross-polarized light microscopy observations of the intensely birefringent lyotropic liquid crystalline solutions of p-BT, p-BNT, and p-BA reveal textures, indicating the liquid crystallinity to be most likely nematic in nature. In general, the solutions appeared almost uniformly birefringent with many indications of extremely fine graininess

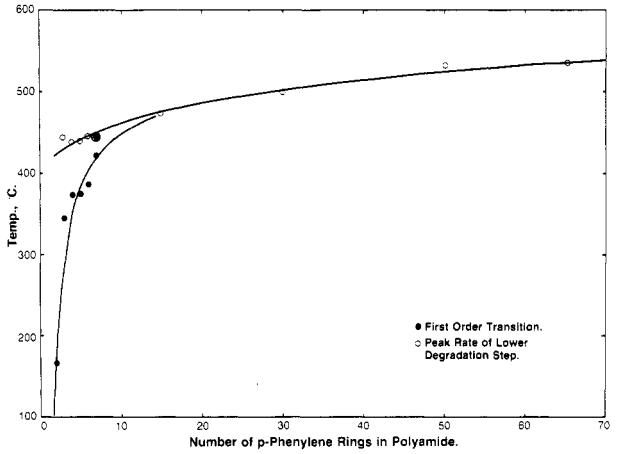

Figure 4. First-order transition and lower degradation temperatures of bulk poly(*p*-benzanilide terephthalamide), plotted as function of the number of aromatic rings (corresponding to the axial ratio) in the polyamide.

in them. Schlieren textures were only seldom observed in small areas, and in these instances only double brushes were observed. Furthermore, in the biphasic solution interval, there were found on occasion nematic droplets which deform during flow, characterized by their distinct Maltese crosses.

Bulk Properties. In this work we were interested in only two bulk properties. Firstly, what is the smallest axial ratio, x_c, below which no thermotropic liquid crystallinity exists, and secondly, at what axial ratio does the WAXD patterns of the oligomers become so similar to those of high-*M* p-BT that they can be assumed to have identical crystal structure.

To determine the thermal characteristics, only the p-BT family was used. It was studied by means of DSC, DTA, and cross-polarized light hot-stage microscopy and in the case of *p*-heptaphenylene hexamide by combining thermostated hot plate with hot-stage microscopy. The results are presented in Figure 4. In several of the DTA scans, it was observed that the degradative weight loss occurs in two steps. Therefore, in the figure the empty data points indicate the peak position of the rate of the lower degradation step in cases where two steps existed and of the only degradation step when only one such step was evident. The hot stage at our disposal is capable of reaching not higher than ~390 °C, and all the first-order transitions we were able to observe by hot-stage microscopy were straightforward melting of crystalline oligomers into an isotropic melt. These transitions were at temperatures far lower than the decomposition temperature. The order of the transitions was inferred by us from the shape of the transition curves in the DSC scans and, when appropriate, from the hot-stage microscope observations.

A melting point of 346 °C was determined by us for the triphenylene diamide. This is in excellent agreement with the values of 343 and 344 °C determined by Gaymans and Harkema[29] for *p*-phenylene bis(benzamide) and dianilinoterephthalamide, respectively. It is obvious that no significant difference exists between the two rigid diamide isomers.

Only the heptaphenylene hexaamide oligomer showed by DSC two very sharp transition peaks appearing as if both are first order in nature. The upper transition was found to coincide with the lower of two degradation steps. Because of the limited range of our hot stage, a thermostated hot plate was used in conjunction with the hot-stage microscope, and the liquid crystalline behavior of this oligomer was clearly evident at the set temperature of 440 °C. Therefore, we conclude that the lower transition of heptaphenylene hexaamide is a transition from crystal to liquid crystal and that the upper transition is an isotropization transition occurring concomitantly with the lower degradation step. The intensity of the transition at 422 °C is rather small, 37 J/g or about 1 kcal/mol aromatic rings. These values are much smaller than usual heats of melting, corroborating the fact that the lower first-order transition of heptaphenylene hexaamide is a crystalline to nematic transition. Here we should recall that from all the monodisperse oligomers, the concentrated solution of only the heptaphenylene hexaamide showed liquid crystallinity. This indicates that this oligomer has an axial ratio sufficient to form liquid crystals. All other oligomers failed to show lyotropic liquid crystallinity or pass through a mesomorphic interval upon heating from the crystal to the isotropic melt. The axial ratio of the heptaphenylene hexaamide is $x = 7$, and that of the next lower homologue is $x = 6$. Therefore, we conclude that liquid crystallinity of short unconnected rodlike polyamide oligomers takes place when $6 < x < 7$. This is in excellent agreement with Flory's prediction[7,8] of $x_c = 6.4$ for rodlike particles.

Table II
WAXD Reflections of p-BT

2θ, deg	*d* spacings, Å	I_{obsd}[a]	*hkl*
20.45	4.34	vs	110
22.73	3.91	vs	200
28.60	3.12	s	004
38.25	2.35	m	211
43.18	2.10	s	006

[a] vs = very strong, s = strong, m = medium intensity.

In order to determine what is the shortest oligomer capable of exhibiting a crystalline X-ray diffraction pattern of a high molecular weight rodlike polyamide, WAXD patterns were obtained of all monodisperse oligomers and several poly(*p*-benzanilide terephthalamide) homologues of increasing molecular weight. These are plotted in panels A–K of Figure 5. Also in the figure are shown the WAXD patterns of poly(*p*-benzamide) in panel L and poly(*p*-phenylene terephthalamide) in panel M. The latter was obtained from drawn and oriented fibers, resulting in better crystalline order and orientation manifested by sharper X-ray reflections. From Figure 5 one can immediately draw the following three conclusions. (a) The oligomer where p-BT pattern first appears is the tetraphenylene triamide in panel C, and the one where low-*M* reflections vanish is the hexaphenylene pentaamide in panel E. (b) The sharpness of the two major reflections of the oligomers having p-BT X-ray pattern (panels D–F) indicates high crystalline perfection and large crystallite size. These characteristics substantially diminish with increased molecular weight (and probable effects of polydispersity) in panels G, H, J, and K. (c) The WAXD patterns of p-BT, p-BA, and p-PT are essentially identical, indicating a great structural similarity, in X-ray terms, among the crystals of these three rodlike polymers.

Because of the remarkable similarity in the position and relative intensity of the WAXD reflections of p-BT, p-BA, and p-PT, it was felt by us that the cell data of p-BT can be calculated using the determinations of Northolt[30,31] for p-PT as a starting point. The five intense reflections of p-BT are listed in Table II together with their *d* spacings, observed intensity, and *hkl* indices. Following Northolt and based on the above, we tentatively propose the cell data for p-BT as indicated in Table III. For two repeat units per cell, the crystallographic density is 1.53 g/cm^3, which is slightly higher than the value of 1.48 g/cm^3 averaged from three pycnometric measurements each on

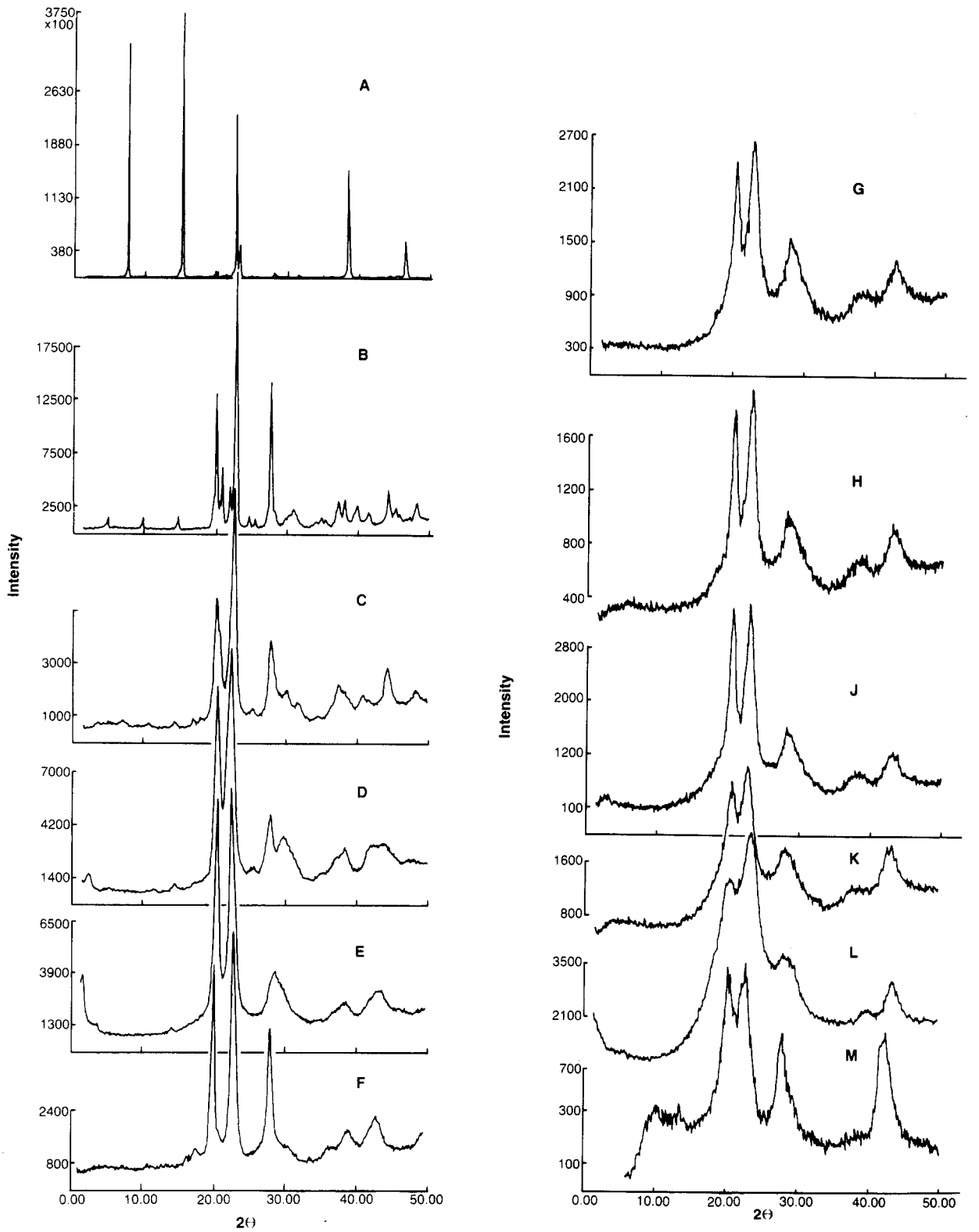

Figure 5. Wide-angle X-ray diffraction patterns of (A) benzanilide; (B) triphenylene diamide; (C) tetraphenylene triamide; (D) pentaphenylene tetraamide; (E) hexaphenylene pentaamide; (F) heptaphenylene hexaamide; (G) poly(*p*-benzanilide terephthalamide), M_w = 1800; (H) same but M_w = 3000; (J) same but M_w = 3900; (K) poly(*p*-benzanilide terephthalamide), M_w = 13 000; (L) poly(*p*-benzamide), M_w = 11 000; (M) poly(*p*-phenylene terephthalamide), Du Pont's Kevlar 29 fibers. The fiber pattern was randomized by mounting on a rotating sample holder. All others were crushed powder, dried overnight in vacuum at 120 °C. Scattering intensities in arbitrary units.

p-BT of M_w = 1800, 7500, and 18 500. The agreement between the calculated and measured densities lends credence to the angle γ being 90° or very close ot it, and the classification of the p-BT crystal as a member of the monoclinic system. By analogy with Northolt[30,31] and Tadokoro and associates,[32] we assume the space group of p-BT to be $P2_1/n$.

Except for benzanilide and *p*-triphenylene diamide,[33,34] we are aware of no crystal structure determination of the monodisperse oligomers of p-BT. The WAXD patterns of these two lowest homologues appear in panels A and B in Figure 5. The pattern of benzanilide is completely different from those of the higher M p-BT homologues. The pattern of *p*-triphenylene diamide starts showing some

Table III
Cell Parameters of p-BT

parameter	value	parameter	value
a	7.82 Å	$\alpha = \beta \simeq \gamma$	90°
b	5.18 Å	no. of chains in cell	2
c	12.6 Å		

similarity to the higher M p-BT's in the position and relative intensity of the three most intense reflections. As one progresses to higher homologues, the polymeric WAXD pattern gradually emerges. When the p-hexaphenylene pentaamide is reached, the pure polymeric pattern of p-BT is obtained. This means that p-BT rodlike chains of $x = 6$ and length of about 37.5 Å produce crystals whose WAXD pattern is that of high-M polymers. Initial indications of such a pattern are obtained at $x = 4$ and $L = 24.5$ Å.

It should be further mentioned that experimental results[30-32,35] as well as theoretical calculations[36,37] show that in both p-PT and p-BA the phenyl rings are not coplanar with the amide groups but are at torsional angles of ±30° relative to the amides. Similar torsional angles between the phenyl rings and amide groups were found also in the case of triphenylene diamide.[33,38] The similarity of the WAXD patterns of p-BT to those of p-BA and p-PT leads us to believe that the torsional angles of the phenyl rings relative to the planes defined by the amide groups in crystalline p-BT are about ±30°, too.

Conclusions

From the results above, we conclude that in dilute solutions the monodisperse oligomers behave as expected from Simha's theory[3-5] with respect to the coefficient a in eq 4 and as expected from Riseman and Ullman's treatment[25] with respect to the coefficient k_H in eq 7. Both of these parameters are dramatically different from the theoretical expectations for rodlike polymers having large axial ratios and from the usually obtained experimental results.

In concentrated solutions, p-BA, p-BT, and p-BNT exhibit lyotropic liquid crystallinity, but only when the axial ratio is larger than 6. The concentration, C_{as}, where a single anisotropic solution is obtained, is significantly different from one another, reflecting the effects of the structural differences and deviations from perfect rodlike behavior among the three families of rodlike polymers. In this case, the differences are far more pronounced than in the case of dilute solutions.

Thermotropic liquid crystallinity is present only in the case of heptaphenylene hexaamide. All shorter monodisperse oligomers exhibited a normal crystal to isotropic melt fit-order transition. Homologues having higher molecular weight showed no first-order transition below the onset of thermal degradation.

The crystal structure of the p-BT polymers is remarkably similar to that of p-BA and p-PT. Monodisperse oligomers of $x \geq 6$ have crystal structures identical with those of the higher M p-BT homologues, but certain similarities with the higher M homologues exist already in the oligomers with $x = 5$, 4, and probably 3. This indicates that a remarkably short rodlike chain is sufficient to develop a polymeric crystal X-ray pattern.

Acknowledgment. I am grateful to D. D. Allmand, M. H. Cozine, C. R. Crosby III, J. T. Dunn, W. B. Hammond, C. Lombardo, M. F. Martin, H. Minor, N. S. Murthy, E. K. Walsh, and K. Zero for their help with various aspects of the experimental work. Illuminating discussions with Professor R. Simha and the late Professor P. J. Flory are acknowledged.

Registry No. p-BT (SRU), 108773-35-9; p-BT (copolymer), 29153-47-7; p-BNT (SRU), 108773-36-0; p-BNT (copolymer), 82914-77-0; p-BA (SRU), 24991-08-0; p-BA (homopolymer), 25136-77-0; benzanilide, 93-98-1; p-triphenylene diamide, 7154-31-6; p-tetraphenylene triamide, 87706-91-0; p-pentaphenylene tetramide, 108773-37-1; p-hexaphenylene pentaamide, 87706-92-1; p-heptaphenylene hexamide, 108773-38-2.

References and Notes

(1) Tanford, C. *Physical Chemistry of Macromolecules*; Wiley: New York, 1961; pp 342–343.
(2) Kirkwood, J. G.; Auer, P. L. *J. Chem. Phys.* **1951**, *19*, 281.
(3) Simha, R. *J. Phys. Chem.* **1940**, *44*, 25.
(4) Mehl, J. W.; Oncley, J. L.; Simha, R. *Science (Washington, D.C.)* **1940**, *92*, 132.
(5) Simha, R. *J. Chem. Phys.* **1945**, *13*, 188.
(6) Flory, P. J. *Proc. R. Soc. London, Ser. A.* **1956**, *234*, 73.
(7) Flory, P. J.; Ronca, G. *Mol. Cryst. Liq. Cryst.* **1979**, *54*, 289.
(8) Flory, P. J.; Ronca, G. *Mol. Cryst. Liq. Cryst.* **1979**, *54*, 311.
(9) Flory, P. J. *Macromolecules* **1978**, *11*, 1141.
(10) Matheson, R. R., Jr.; Flory, P. J. *Macromolecules* **1981**, *14*, 954.
(11) Aharoni, S. M. *J. Appl. Polym. Sci.* **1980**, *25*, 2891.
(12) Aharoni, S. M. *J. Polym. Sci., Polym. Phys. Ed.* **1981**, *19*, 281.
(13) Yamazaki, N.; Matsumoto, M.; Higashi, F. *J. Polym. Sci., Polym. Chem. Ed.* **1975**, *13*, 1373.
(14) Aharoni, S. M. *Macromolecules* **1983**, *16*, 1722.
(15) Aharoni, S. M. *Macromolecules* **1986**, *19*, 426.
(16) Schaefgen, J. R.; Foldi, V. S.; Logullo, F. M.; Good, V. H.; Gulrich, L. W.; Killian, F. L. *Polym. Prepr.—Am. Chem. Soc., Div. Polym. Chem.* **1976**, *17*(1), 60.
(17) Tsvetkov, V. N.; Kudriavtsev, G. I.; Shtennikova, I. N.; Peker, T. V.; Zakharova, E. N.; Kalmykova, V. D.; Volokhina, A. V. *Europ. Polym. J.* **1976**, *12*, 517.
(18) Arpin, M.; Strazielle, C. *Polymer* **1977**, *18*, 591.
(19) Lavrenko, P. N.; Okatova, O. V. *Polym. Sci. USSR (Engl. Transl.)* **1979**, *21*, 406.
(20) Tsvetkov, V. N.; Andreeva, L. N.; Lavrenko, P. N.; Okatova, O. V.; Beliaeva, E. V.; Bilibin, A. Yu.; Skororkhodov, S. S. *Eur. Polym. J.* **1985**, *21*, 933.
(21) Aharoni, S. M.; Wertz, D. H. *J. Macromol. Sci.—Phys.* **1983**, *B22*, 129.
(22) Baird, D. G.; Smith, J. K. *J. Polym. Sci., Polym. Chem. Ed.* **1978**, *16*, 61.
(23) Baird, D. G.; Ballman, R. L. *J. Rheol.* **1979**, *23*, 505.
(24) Huggins, M. L. *J. Am. Chem. Soc.* **1942**, *64*, 2716.
(25) Riseman, J.; Ullman, R. *J. Chem. Phys.* **1951**, *19*, 578.
(26) Simha, R. *J. Res. Natl. Bur. Stand.* **1949**, *42*, 409.
(27) Riseman, J.; Kirkwood, J. G. *J. Chem. Phys.* **1950**, *18*, 512.
(28) Aharoni, S. M. *J. Macromol. Sci.—Phys.* **1982**, *B21*, 105.
(29) Gaymans, R. J.; Harkema, S. *J. Polym. Sci., Polym. Phys. Ed.* **1977**, *15*, 587.
(30) Northolt, M. G.; Van Aartsen, J. J. *J. Polym. Sci., Polym. Lett. Ed.* **1973**, *11*, 333.
(31) Northolt, M. G. *Eur. Polym. J.* **1974**, *10*, 799.
(32) Tashiro, K.; Kobayashi, M.; Tadokoro, H. *Macromolecules* **1977**, *10*, 413.
(33) Harkema, S.; Gaymans, R. J. *Acta Crystallogr., Sect. B* **1977**, *B33*, 3609.
(34) Adams, W. W.; Fratini, A. V.; Wiff, D. R. *Acta Crystallogr., Sect. B* **1978**, *B34*, 954.
(35) Tadokoro, H. *Structure of Crystalline Polymers*; Wiley-Interscience: New York, 1979; pp 396–401.
(36) Hummel, J. P.; Flory, P. J. *Macromolecules* **1980**, *13*, 479.
(37) Erman, B.; Flory, P. J.; Hummel, J. P. *Macromolecules* **1980**, *13*, 484.
(38) Calabrese, J. C.; Gardner, K. H. *Acta Crystallogr., Sect. C* **1985**, *C41*, 389.